PHYSICAL REVIEW B VOLUME 58, NUMBER 12 15 SEPTEMBER 1998-II

Oxygen isoelectronic impurities in ZnTe: Photoluminescence and absorption spectroscopy

M. J. Seong, I. Miotkowski, and A. K. Ramdas
Department of Physics, Purdue University, West Lafayette, Indiana 47907

(Received 16 March 1998)

Oxygen substituting for Te in ZnTe is an isoelectronic impurity that traps excitons. The recombination radiation and absorption spectra attributed to isolated oxygen centers exhibit a no-phonon line accompanied by emission of multiple phonons. The two resulting spectra are ''mirror images'' of each other in energy with respect to that of the no-phonon line. Photoluminescence and absorption measurements on specimens with significantly higher oxygen concentration disclosed additional spectral features with four no-phonon lines, all displaced to lower energies with respect to that of isolated oxygen. Photoluminescence spectra of the present no-phonon lines show a temperature dependence characteristic of exchange coupling between an electron and a hole. Selective excitation with photon energies less than that of the no-phonon line of isolated oxygen permitted a clear observation of the features free from the phonon sidebands of isolated oxygen. These features, including phonon replicas, appear to be due to excitons bound to oxygen pairs, with different OO separations. [S0163-1829(98)03236-6]

I. INTRODUCTION

In the context of donors, acceptors, and electrically inactive impurities in semiconductors, there exists a fascinating subset designated as *isoelectronic*.[1] An impurity replacing a host atom with the same valence orbitals is labeled isoelectronic. Often localized states in the forbidden band occur due to excitons bound to such centers. Nitrogen replacing phosphorus in GaP is an example of such a trap.[2] The bonding scheme of substitutional donors or acceptors in the tetrahedrally coordinated semiconductors is based on the ''sp^3'' hybridized covalent bond. For example, consider GaP doped with Zn and S. Zn replacing Ga is an acceptor and S replacing P is a donor. Besides acceptor-bound holes and donor-bound electrons, one can encounter in such crystals donor-bound and acceptor-bound excitons,[3] the excitons being bound to the neutral donors and acceptors by a van der Waals interaction. On the other hand, N and Bi, replacing P in GaP, have the *same* number of valence electrons as P does, but they can trap a charge carrier by a non-Coulombic, short-range impurity potential resulting from the substantial electronegativity difference between N and P (or Bi and P). The impurity, originally neutral, then acquires a charge relative to the lattice. Bound excitons occur when the Coulomb field of this charge binds a second charge carrier of the opposite sign, localized in a large hydrogenlike orbital. A center like N (Bi) is called an isoelectronic acceptor (donor), according to the type of the charge carrier (electron or hole) bound to it in a hydrogenic orbit.[4] The exciton binding energy of isoelectronic impurities ranges from tens to hundreds of meV, depending on the impurity and the host. Isoelectronic impurities have been fascinating subjects of study in view of the underlying physics manifested in their photoluminescence (PL),[2] absorption,[5] PL excitation,[6] and localized vibrational modes.[7] Isoelectronic traps, with their high radiative recombination efficiency, play an important role in the optoelectronic device applications, e.g., light-emitting diodes and semiconductor laser diodes.[8,9]

A remarkable spectrum due to oxygen isoelectronic impurity in ZnTe was observed in PL as well as in absorption by Dietz *et al.*[10] A no-phonon line appears both in absorption and in emission. At low temperatures, the no-phonon line in PL is accompanied by phonon replicas on the lower-energy side, representing the creation of a quantum of LO, TO, LA, and TA phonons as well as multiples of the LO phonon accompanied by the creation of TO, LA, and TA phonons; in absorption, in contrast, they are ''mirrored'' on the high-energy side of the no-phonon line. Merz[11] observed a shift for the no-phonon lines in the PL spectrum associated with excitons bound to isoelectronic oxygen centers when O^{18} is replaced with O^{16}. An isotope shift of the no-phonon line results from the zero-point vibrations of the ground and excited states of an electronic transition being shifted to different extents by the electron-phonon interaction. From the absence of an orientation dependence of the Zeeman splitting, he concluded that the point defect has spherical symmetry. The analogous case of nitrogen isoelectronic impurity in GaP is equally instructive in this context. Comprehensive experimental and theoretical studies of the spectroscopy of nitrogen traps in GaP have been reported;[2,4,12–17] signatures of excitons bound to isolated nitrogen atoms, substituted for phosphorus atoms, as well as NN lines corresponding to excitons bound to pairs of nitrogen atoms have been observed.[2,14] The low solubility limit of oxygen in a ZnTe crystal grown from a melt, $\sim 10^{17}$ oxygen atoms/cm^3,[15] combined with the presence of the strong phonon side bands of the no-phonon lines of isolated oxygen, has presumably contributed to the difficulty in observing the ''OO lines.''

In the course of a general program on II-VI semiconductors and their quantum well structures (in particular their optical characterization with respect to group IIA, 3d transition metal ions, and group VI impurities) we have recently reinvestigated oxygen doped ZnTe. We report in this paper our successful observation of OO pair spectra in ZnTe. We compare and contrast the similarities and differences between the isolated oxygen and OO centers with respect to their PL and absorption spectra.

0163-1829/98/58(12)/7734(6)/$15.00

II. EXPERIMENT

Single crystals of ZnTe were grown using the Bridgman technique. Oxygen doping was achieved with the addition of a small amount of ZnO powder to the ZnTe source material inside a quartz ampoule. For absorption measurement both sides of the sample were polished to a surface roughness of $\sim 0.5 \mu$m. Cleaved as well as polished specimens were used for PL measurement.

The PL spectra were recorded with a SPEX (Model 14018) 0.85 m double grating monochromator.[18] The samples were excited using the 5145 Å line from a Coherent Ar^+ laser[19] or the 5682 Å line from a Spectra-Physics Kr^+ laser.[20] For a selective excitation of the PL from OO centers, the 6328 Å line from a Spectra-Physics He-Ne laser or an appropriate line from a Coherent tunable dye laser with Rhodamine 6G was used. The sample temperature was controlled from 1.5 K to 300 K in a Janis 10 DT (Ref. 21) cryostat and an RCA (type C31034A) photomultiplier was used as a detector. Absorption measurements were carried out using a 650 W tungsten halogen lamp as a white light source, the sample being cooled in a Janis SuperTran[21] cryostat. The transmitted spectra were recorded with a SPEX (Model 1403) 0.85 m double grating monochromator and an RCA (type C31034A) photomultiplier was used as a detector.

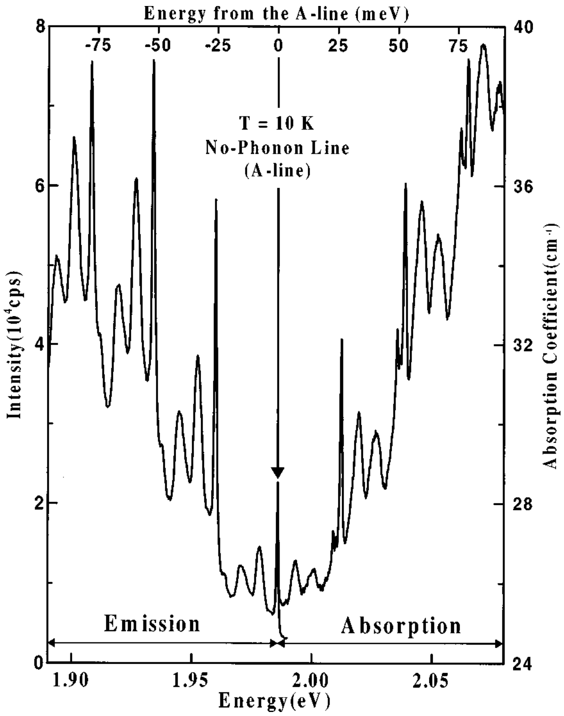

FIG. 1. Absorption spectrum and its ''mirror image'' in the emission spectrum of excitons bound to the isolated oxygen isoelectronic impurity in ZnTe. The dipole allowed no-phonon line (*A* line) at 1.986 eV is common to both spectra. The sharp LO phonon replicas are separated by 26 meV. The scale on the top of the figure emphasizes the energy separations of the phonon replicas with respect to the *A* line, plus in absorption and minus in emission.

III. RESULTS AND DISCUSSION

A. Isolated oxygen center

In Fig. 1 the absorption spectrum and its ''mirror image'' in the emission spectrum of oxygen center in ZnTe is displayed; the two spectra are mirrored about the no-phonon line (*A* line) at 1.986 eV observed in both absorption and emission. The *A* line is accompanied by phonon replicas representing the creation of a quantum of LO, TO, LA, and TA phonon as well as multiples of the LO phonon, each in turn accompanied by TO, LA, and TA signatures in both recombination (PL) and absorption spectra. In Fig. 2 the temperature dependence of the PL spectrum is shown. As the temperature is reduced below ~ 5 K, a new emission line (*B* line) is observed at an energy 1.5 meV lower than that of the *A* line. At 1.5 K, the *B* line completely dominates the *A* line and all the observed phonon replicas are then those associated with the *B* line and shifted accordingly. The energies of the *A* and *B* transitions of the oxygen center and their phonon replicas in absorption and emission are listed in Table I.

For a zinc-blende crystal such as ZnTe, the excited state of an isoelectronic trap is the $J=1$ and $J=2$ doublet resulting from the exchange coupling of a $j_h=\frac{3}{2}$ hole with a $j_e=\frac{1}{2}$ electron, the doublet splitting being 1.5 meV for ZnTe:O. Transitions from the $J=1$ upper level to the $J=0$ ground state are electric dipole allowed; the strong line (*A* line) seen in PL spectra above ~ 5 K is attributed to such a transition, viz., the 1.986 eV no-phonon line in Fig. 1. Transitions from the $J=2$ lower level of the doublet to the $J=0$ ground state are electric dipole forbidden. However, as the temperature is reduced below 5 K, the upper level is thermally depopulated and a new emission line (*B* line) is observed originating from the $J=2$ state. That the dipole forbidden *B* line is observed at all is partly due to phonon

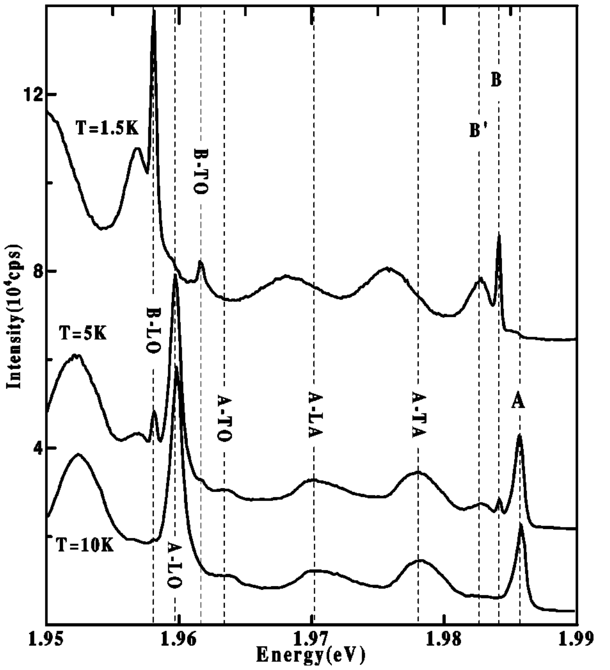

FIG. 2. Temperature dependence of the PL spectrum of ZnTe:O excited with the 5682 Å line from a Kr^+ laser. The spectra at different temperatures are vertically shifted for clarity and the intensities at 5 K and 1.5 K are multiplied by 2 and 20, respectively.

TABLE I. Measured energy positions of isolated oxygen no-phonon lines and their phonon replicas in ZnTe and no-phonon lines of oxygen pairs.

Center	Line	Peak position (eV)	Phonon energy (meV)
isolated oxygen	O(A)	1.9857	
	O(A)− TA	1.9779	
	O(A)−LA	1.9701	TA=7.9±0.5
	O(A)−TO	1.9634	
	O(A)−LO	1.9597	
	O(A)+TA	1.9932	LA=15.6±0.5
	O(A)+LA	2.0008	
	O(A)+TO	2.0088	
	O(A)+LO	2.0121	TO=22.7±0.4
	O(B)	1.9842	
	O(B)−TA	1.9758	
	O(B)−LA	1.9681	LO=26.2±0.2
	O(B)−TO	1.9616	
	O(B)−LO	1.9581	
oxygen pairs	OO_1(A)	1.9419	
	OO_2(A)	1.9456	
	OO_3(A)	1.9697	TA=7.9±0.5
	OO_4(A)	1.9738	LA=15.2±0.4
	OO_1(B)	1.9404	TO=22.3±0.3
	OO_2(B)	1.9441	LO=26.1±0.1
	OO_3(B)	1.9682	
	OO_4(B)	1.9724	

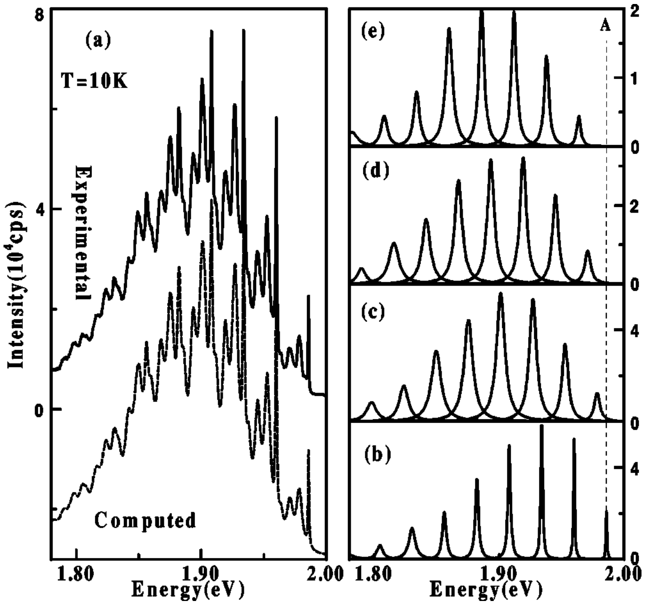

FIG. 3. PL spectrum of the isolated oxygen center in ZnTe and its resolution into Lorentzian peaks with all phonon modes taken into account based on the Franck-Condon principle. (a) Experimentally observed PL spectrum and fitted curve using its resolution into Lorentzian peaks. (b) LO phonon component of the phonon side bands of the isolated oxygen center in ZnTe. The first peak from the right is the no-phonon line. (c) TA phonon contribution to the phonon sidebands with the first peak from the right being the TA phonon replica of the no-phonon A line (A-TA), the second being A-(TA+LO), the third A-(TA+2LO), etc. (d) Contributions of the A-LA, A-(LA+LO), A-(LA+2LO), etc., phonon replicas. (e) Contributions of the A-TO, A-(TO+LO), A-(TO+2LO), etc., phonon replicas.

assisted mixing of the $J=2$ and $J=1$ states and partly due to a relaxation of the selection rules presumably caused by residual strains around the oxygen center.[1] The broad band labeled B' was interpreted by Dietz *et al.*[10] as an acoustic phonon wing associated with the transition originating at the $J=2$ state via a virtual transition to the $J=1$ state accompanied by the emission of acoustic phonons. Recently, Burki *et al.*[22] argued that pairs composed of isoelectronic impurity and a neutral acceptor with different distances are responsible for the broad band B'.

The probabilities of the individual vibronic transitions and therefore the line intensities as well as the general structure of the spectrum are explained on the basis of the *Franck-Condon principle*;[23] the lattice coordinates R do not change significantly during the optical transition, allowing the electronic transition to occur mostly vertically in a configuration coordinate diagram. The probability for an optical transition at a center is then proportional to the square of the dipole matrix element $\langle \psi_e \chi_{e,m} | \mathbf{r} | \psi_g \chi_{g,n} \rangle$, where ψ is an electronic wave function, χ is a vibrational wave function in each electronic state, $\mathbf{r}$ is the electronic coordinate, and the subscripts e and g stand for electronic excited and ground states, respectively. The electric dipole moment is assumed to be independent of the nuclear coordinate R and hence the matrix element can be factored into $\langle \psi_e | \mathbf{r} | \psi_g \rangle \langle \chi_{e,m} | \chi_{g,n} \rangle$. Thus the optical line shape is determined by the vibrational overlap integral. At low temperatures, the transition probability from the zeroth vibrational level of the electronic ground state to the mth vibrational level of the electronic excited state is given by $W_{m0}=S^m e^{-S}/m!$, the most probable number of phonons being $m \approx S$. The above argument applies also to the emission spectrum, originating from the zeroth vibrational level of the electronic excited state to the nth vibrational level of the electronic ground state, resulting in the transition probability $W_{0n}=S^n e^{-S}/n!$. According to this model, the absorption and emission spectra should be mirror images of each other about the common no-phonon line. In Fig. 3 the experimentally observed PL spectrum of the isolated oxygen center in ZnTe and its resolution into Lorentzian peaks, taking into account the contributions of all the relevant phonon types, are displayed. The fitted spectrum consists of four classes of phonon components, viz., TA, LA, TO, and LO, as shown in Figs. 3(b)–3(e). The integrated intensities of the LO phonon overtones show good agreement with that predicted by W_{0n} with $S_{\mathrm{LO}} \approx 3.4$. All the phonon components superimpose in the sum to faithfully reproduce all the detailed features of the experimental data [Fig. 3(a)].

B. OO centers

In Fig. 4 PL spectra of a ZnTe crystal doped with oxygen, excited with the 6328 Å line from a He-Ne laser, are shown. Since excitation energy thus selected is lower than that of the isolated oxygen no-phonon lines, excitons bound to isolated oxygen centers are not excited. Therefore, the strong phonon side bands of the isolated oxygen no-phonon lines are not

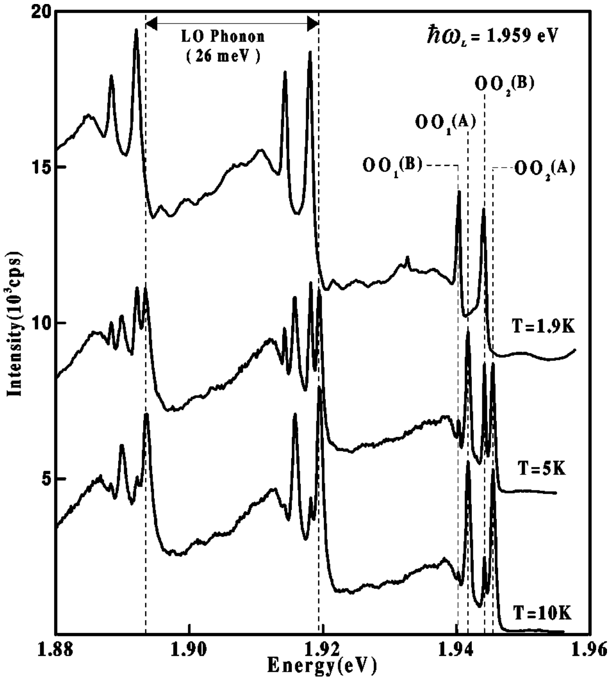

FIG. 4. PL spectrum of excitons bound to OO pairs in ZnTe as a function of temperature. The spectrum is selectively excited with the 6328 Å line from a He-Ne laser.

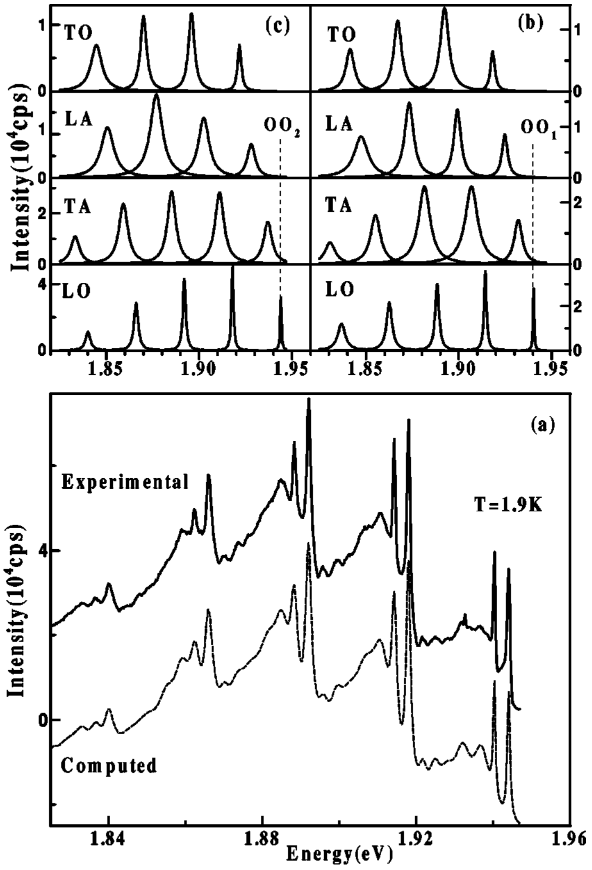

FIG. 5. Experimentally observed PL spectrum of OO_1 and OO_2 at 1.9 K analyzed with the same procedure as that employed for the isolated oxygen center (Fig. 3). (a) Experimental data compared with the sum of all the phonon components. (b) Each phonon component of OO_1. (c) Each phonon component of OO_2.

generated. New lines $OO_1(A)$, $OO_1(B)$, $OO_2(A)$, and $OO_2(B)$ with their phonon side bands are clearly observed. The two lines $OO_1(A)$ and $OO_2(A)$ can be interpreted as dipole allowed transitions of excitons bound to *pairs of oxygen atoms with different OO separations*. On the basis of their temperature dependence, $OO_1(B)$ and $OO_2(B)$ can be attributed to the dipole forbidden transitions. In contrast to the temperature dependence of PL spectra of the isolated oxygen in Fig. 2, the $OO_1(B)$ and $OO_2(B)$ lines can be clearly seen already at 10 K and the intensity of $OO_2(B)$ is comparable to that of $OO_2(A)$ even at 5 K. This may be attributed to lowered local symmetry in these centers resulting in relaxation of the selection rule that the transition from the $J=2$ states are forbidden. In Fig. 5 the experimental PL data at 1.9 K and its resolution into the Lorentzian peaks (as was carried out for the isolated oxygen center in Fig. 3) are displayed. The energies of TA, LA, TO, and LO phonons involved are the same as those for isolated oxygen center. $OO_1(A)$ and $OO_2(A)$ are observed in the absorption spectrum along with their phonon replicas as shown in Fig. 6. There are additional features, labeled $OO_3(A)$ and $OO_4(A)$, around the LO phonon replicas of $OO_1(A)$ and $OO_2(A)$. They are presumably OO lines corresponding to larger separations between the oxygen impurities than in those responsible for OO_1 and OO_2 since OO lines would converge to the *A* line of the isolated oxygen center as the OO distance increases.

In order to observe the PL spectrum corresponding to the OO_3 and OO_4 features in the absorption spectrum, we selectively excited the sample with a laser light of energy ($\hbar\omega_L$), larger than the energy of $OO_4(A)$ but smaller than those for the isolated oxygen no-phonon lines. In Fig. 7 PL spectra excited with $\hbar\omega_L=1.982$ eV from a tunable dye laser are displayed. $OO_3(A)$ and $OO_4(A)$ are observed at the same energies as those of the corresponding absorption features. From their temperature dependence, $OO_3(A)$ and $OO_4(A)$ can be attributed to dipole allowed transitions, while $OO_3(B)$ and $OO_4(B)$ are the dipole forbidden counterparts. In these centers, the selection rule for the transition from the $J=2$ excited state to the $J=0$ ground state is relaxed to some extent presumably due to the lowered local symmetry and the intensities of $OO_3(B)$ and $OO_4(B)$ are larger than those of $OO_3(A)$ and $OO_4(A)$, respectively, even at 10 K. The lowered local symmetry at OO_3 may have caused the feature $OO_3(B)^*$ to split off from the $OO_3(B)$ line. The energies of the no-phonon lines of OO_1, OO_2, OO_3, and OO_4 as well as the phonon energies associated with their phonon replicas in absorption and emission are listed in Table I.

The following arguments may be cited in support of the above interpretation of the OO lines. (i) They are observed only in ZnTe crystals that exhibit the isolated oxygen lines. (ii) The $J=1$ and $J=2$ splittings of all the OO lines are the same as that for the isolated oxygen center. (iii) Excitonic molecules bound to an isolated oxygen center can be ruled out as their underlying cause since they are observed through the selective excitation even in the absence of excitons bound to the isolated oxygen centers. If they were excitonic molecules bound to isolated oxygen centers, one would have expected selection rules and temperature dependence differ-

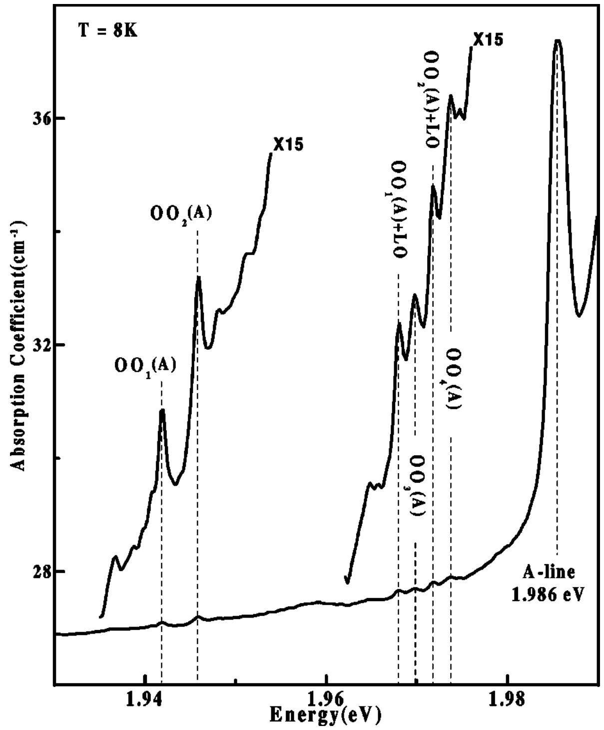

FIG. 6. Absorption spectrum showing the no-phonon OO lines in ZnTe and their phonon replicas. Note the no-phonon $OO_3(A)$ and $OO_4(A)$ features near the LO phonon replicas of $OO_1(A)$ and $OO_2(A)$.

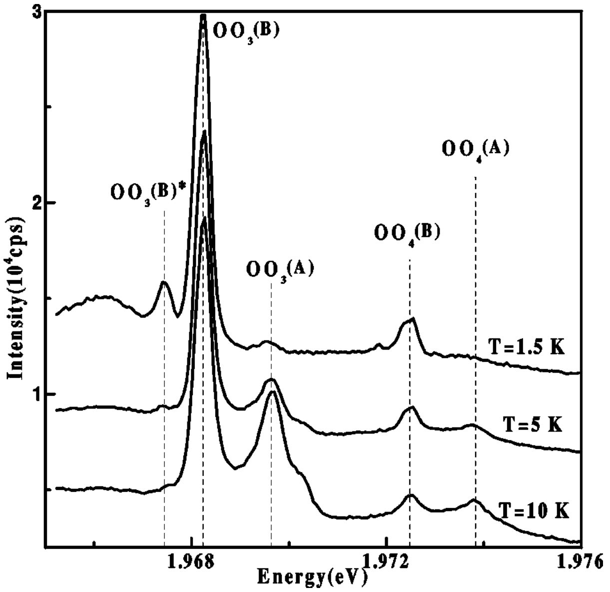

FIG. 7. OO_3 and OO_4 no-phonon OO lines, excited in the PL spectrum of ZnTe with a tunable dye laser ($\hbar\omega_L = 1.982$ eV), recorded at 1.5 K, 5 K, and 10 K.

ent from those characterizing our data; besides, the luminescence features associated with excitonic molecule and single exciton (both bound to isolated oxygen) should have appeared together.[24] (iv) Their observation as mirror images in both emission and absorption with respect to their no-phonon lines clearly demonstrates that they are not phonon replicas of the isolated oxygen feature. (v) It is highly unlikely that they are due to an isoelectronic impurity other than oxygen because their binding energies are larger than that of the isolated oxygen-bound exciton. Since oxygen has the largest electronegativity difference with respect to Te among the group VI elements (O, S, and Se), excitons would be more tightly bound to the oxygen center than to the other isoelectronic centers. (vi) The energy range in which the four OO lines occur with respect to that of the isolated oxygen center, on the one hand, and their convergence to the isolated oxygen line, on the other hand, are additional significant arguments in support of the new lines being due to OO centers with differing pair distances. (vii) There is thermalization within the $J=1$ and $J=2$ lines for each OO_n, as there is for the isolated oxygen A and B lines, but not between the different OO_n lines. This makes it most unlikely that the same center is involved in all the lines, such as would be the case if excited states of a center were involved.

IV. CONCLUDING REMARKS

The strong interaction between the electron of the bound exciton and the zone center (Γ) LO phonon (Fröhlich interaction), on the one hand, and the unique aspects of the short-range potential of the isoelectronic impurity, on the other hand, are responsible for the rich vibronic spectra of the oxygen centers in ZnTe.[4] In addition, the lattice deformation around the impurity in its electronic excited state compared to that in the electronic ground state, both considered in the configuration coordinate model, provides the microscopic picture for the vibronic structure. The model for excitons bound to isoelectronic acceptors and donors proposed by Hopfield *et al.*[4] has proved very successful in qualitatively explaining many properties of isoelectronic impurities. A recent quantitative study of the binding energies of isoelectronic impurities in II-VI semiconductors by Sohn and Hamakawa[25] based on this model shows good agreement with the experimental data in the literature. In this context it is of interest to explore the excited states of the isolated oxygen center as well as those of the OO pairs with PL excitation and far infrared exciton absorption spectroscopy.[26]

In contrast to the case of excitons bound to neutral acceptors, where the exchange interaction between three particles (two holes and an electron) leads to the characteristic triplet of no-phonon lines corresponding to $J=\frac{1}{2},\frac{3}{2},\frac{5}{2}$ states and ''two hole'' transitions,[27] excitons bound to isoelectronic acceptors (donors) are characterized by $J=1$ and $J=2$ states due to exchange interaction between two particles (a hole and an electron). Clear evidence for the $J=1$ and $J=2$ states of the excitons bound to the isoelectronic OO centers has been obtained in this work. Lowered local symmetry of the OO centers resulting in additional no-phonon lines such as $OO_3(B)^*$ provides motivation for the investigation of the symmetry properties of the oxygen centers with Zeeman effect,[2] piezospectroscopy,[28] and polarized luminescence measurements.[29]

ACKNOWLEDGMENTS

The authors acknowledge support from National Science Foundation Grant No. DMR 92-21390 (Materials Research Group) and Grant No. 94-00415 (Materials Research Science and Engineering Center).

[1] W. Czaja, in *Festkörprobleme XI*, edited by Marburg O. Madelung (Pergamon, Oxford, 1971), pp. 65–85.

[2] D. G. Thomas and J. J. Hopfield, Phys. Rev. **150**, 680 (1966).

[3] P. J. Dean and D. C. Herbert, in *Excitons*, edited by K. Cho (Springer, Berlin, 1979), pp. 55–182.

[4] J. J. Hopfield, D. G. Thomas, and R. T. Lynch, Phys. Rev. Lett. **17**, 312 (1966).

[5] V. Slusarenko, Y. Burki, W. Czaja, and H. Berger, Phys. Status Solidi B **161**, 897 (1990).

[6] C. Caneau, M. Schneider, and J. F. Rommeluere, J. Phys. Chem. Solids **42**, 729 (1981).

[7] M. Dean Sciacca, A. J. Mayur, N. Shin, I. Miotkowski, A. K. Ramdas, and S. Rodriguez, Phys. Rev. B **51**, 6971 (1995).

[8] L. A. Kolodziejski, R. L. Gunshor, Q. Fu, D. Lee, A. V. Nurmikko, J. M. Gonsalves, and N. Otsuka, Appl. Phys. Lett. **52**, 1080 (1988).

[9] Q. Fu, D. Lee, A. V. Nurmikko, L. A. Kolodziejski, and R. L. Gunshor, Phys. Rev. B **39**, 3173 (1989).

[10] R. E. Dietz, D. G. Thomas, and J. J. Hopfield, Phys. Rev. Lett. **8**, 391 (1962).

[11] J. L. Merz, Phys. Rev. **176**, 961 (1968).

[12] D. G. Thomas, M. Gershenzon, and J. J. Hopfield, Phys. Rev. **131**, 2397 (1963).

[13] Y. Yafet and D. G. Thomas, Phys. Rev. **131**, 2405 (1963).

[14] D. G. Thomas, J. J. Hopfield, and C. J. Frosch, Phys. Rev. Lett. **15**, 857 (1965).

[15] J. D. Cuthbert and D. G. Thomas, Phys. Rev. **154**, 763 (1967).

[16] J. J. Hopfield, P. J. Dean, and D. G. Thomas, Phys. Rev. **158**, 748 (1967).

[17] Roger A. Faulkner, Phys. Rev. **175**, 991 (1968).

[18] SPEX Industries Inc., 3880 Park Ave., Metuchen, NJ 08840.

[19] Coherent Inc., 5100 Patrick Henry Dr., P.O. Box 54980, Santa Clara, CA 95054.

[20] Spectra-Physics Lasers, 1330 Terra Bella Avenue, P.O. Box 7013, Mountain View, CA 94039.

[21] Janis Research Inc., P.O. Box 696, 2 Jewel Dr., Wilmington, MA 01887-0696.

[22] Y. Burki, W. Czaja, V. Capozzi, and P. Schwendimann, J. Phys.: Condens. Matter **5**, 9235 (1993).

[23] B. Henderson and G. F. Imbusch, *Optical Spectroscopy of Inorganic Solids* (Oxford University Press, Oxford, 1989).

[24] J. L. Merz, R. A. Faulkner, and P. J. Dean, Phys. Rev. **188**, 1228 (1969).

[25] S. H. Sohn and Y. Hamakawa, Phys. Rev. B **46**, 9452 (1992).

[26] M. L. W. Thewalt, D. Labrie, and T. Timusk, Solid State Commun. **53**, 1049 (1985).

[27] H. Venghaus and P. J. Dean, Phys. Rev. B **21**, 1596 (1980).

[28] H. Mathieu, L. Bayo, J. Camassel, and P. Merle, Phys. Rev. B **22**, 4834 (1980).

[29] C. C. Klick and W. D. Compton, J. Phys. Chem. Solids **7**, 170 (1958).